AL008 Enhances Myeloid Antitumor Function by Inhibiting SIRPα Signaling and Activating Fc Receptors

Jingping Yang, Isaiah Deresa, Wei-Hsien Ho, Hua Long, Daniel Maslyar, Arnon Rosenthal, Spencer C. Liang, and Andrew Pincetic

Antagonizing the CD47–signal regulatory protein (SIRP)α pathway, a critical myeloid checkpoint, promotes antitumor immunity. In this study, we describe the development of AL008, a pan-allelic, SIRPα-specific Ab that triggers the degradation of SIRPα and, concurrently, stimulates FcγR activation of myeloid cells through an engineered Fc domain. AL008 showed superior enhancement of phagocytosis of tumor cells opsonized with antitumor Ag Abs compared with another SIRPα Ab tested. Unlike ligand-blocking SIRPα Abs, AL008 demonstrated single-agent activity by increasing tumor cell engulfment by human monocyte-derived macrophages even in the absence of opsonizing agents. This effect was due to enhanced Fc function, as blocking FcγR2A abrogated AL008-mediated phagocytic activity. AL008 also promoted human monocyte-derived dendritic cell–mediated T cell proliferation. In humanized mouse models, AL008 induced internalization of SIRPα and increased expression of CD86 and HLA-DR on human tumor-associated macrophages, confirming that the mechanism of action is retained in vivo. Monotherapy treatment with AL008 significantly reduced tumor growth in humanized mice implanted with human MDA-MB-231 tumor cells. AL008 also significantly potentiated the effects of T cell checkpoint blockade with anti–programmed death ligand-1 in syngeneic tumor models. This dual and specific mechanism of AL008, to our knowledge, provides a novel therapeutic strategy for targeting myeloid cells for immune activation. ***The Journal of Immunology*****, 2023, 210: 204–215.**

Macrophages are a heterogeneous group of tissue-resident myeloid cells and typically represent a predominant immune cell population in tumors (1, 2). Studies on several different cancer types have established that a greater density of tumor-associated macrophages (TAMs) correlates with worse prognosis for patients, which is indicative of their protumorigenic role in disease (1). Under normal physiologic conditions, macrophages maintain tissue homeostasis by sensing injury or infection and executing the programmed removal of damaged, aged, or malignant cells. Tumor cells escape innate immune surveillance through the expression of ligands or factors that negatively regulate these functions by macrophages (3).

One such immune checkpoint is the CD47–signal regulatory protein (SIRP)α interaction, which serves as a "do-not-eat-me" signal to shield cells from macrophage-mediated phagocytosis (4, 5). CD47 is a transmembrane glycoprotein overexpressed in many tumors, and it delivers an inhibitory signal to myeloid cells through its interaction with SIRPα, a myeloid checkpoint receptor (6). SIRPα is a type I transmembrane protein that upon activation recruits Src homology 2 domain–containing protein tyrosine phosphatases 1 (SHP-1) and 2 (SHP-2) to inhibit signaling of multiple activating receptors. Signaling through SIRPα leads to reduced phagocytosis, Ag presentation, and general inhibition of the immune response (7). SIRPα also has CD47-independent activity through interactions with surfactant proteins A and D to inhibit phagocytosis (8). Numerous studies associate high CD47 or SIRPα expression with poor survival in certain cancers (6, 9), consistent with the CD47/SIRPα axis playing a role in immune evasion. Furthermore, blockade of the CD47–SIRPα interaction reduces tumor growth in multiple preclinical models (9–12). Thus, targeting the CD47/SIRPα axis is a promising therapeutic intervention to promote antitumor immunity.

Although recent clinical data with CD47-targeted therapies have demonstrated clinical responses in combination with antitumor Ag Abs or chemotherapy in hematologic cancers (13), more modest responses were observed in solid tumors (14). This may reflect the limitations of targeting CD47. The broad tissue distribution of CD47 necessitates high doses of drug to overcome the large peripheral Ag sink and engage sufficient target in the tumor. Higher doses of Ab increase the risk of Ab-mediated clearance of healthy cells (i.e., RBCs and platelets), as evidenced by dose-limiting toxicities that include anemia and thrombocytopenia in several clinical trials (13, 15, 16).

In addition to its well-known role in inhibiting phagocytosis, CD47 has been implicated in T cell function through its interaction with SIRPγ (17), a SIRP homolog unique to primates that binds CD47 with a lower affinity than SIRPα (18, 19). Recently, nonselective anti-SIRPα/γ Abs blocking CD47 interaction were shown to impair human T cell activation, proliferation, and endothelial transmigration, whereas selective SIRPα blockade preserved and enhanced T cell responses (10).

Targeting SIRPα with mAbs has distinct advantages compared with targeting CD47. First, SIRPα exhibits a more restricted expression pattern compared with CD47, with macrophages and dendritic

Alector, Inc., South San Francisco, CA

ORCIDs: 0000-0001-8275-6669 (D.M.); 0000-0002-5813-4568 (A.P.).

Received for publication February 23, 2022. Accepted for publication November 2, 2022.

This work was supported by Alector, Inc.

A.P., S.C.L., H.L., D.M., and A.R. conceptualized the work; A.P., S.C.L., and H.L. are responsible for the methodology; A.P., J.Y., I.D., W.-H.H., and S.C.L. performed experiments and analyzed data; A.P. and S.C.L. wrote the original draft of the manuscript; and D.M. and A.R. contributed to reviewing and editing the manuscript.

Address correspondence and reprint requests to Dr. Andrew Pincetic, Alector, Inc., 131 Oyster Point Boulevard, Suite 600, South San Francisco, CA 94080. E-mail address: andrew.pincetic@alector.com

The online version of this article contains supplemental material.

Abbreviations used in this article: ADCC, Ab-dependent cellular cytotoxicity; ADCP, Ab-dependent cellular phagocytosis; gRNA, guide RNA; hu, human; NSLF, N325S/L328F; PD-1, programmed death-1; PD-L1, programmed death-ligand 1; PTX, paclitaxel; SIRP, signal-regulatory protein; PBS/T, PBS/0.05% Tween 20; TAM, tumor-associated macrophage; Tg, transgenic.

cells defining the highest expressing cell populations (20). Second, a SIRPα-specific Ab permits antagonizing the inhibitory CD47–SIRPα pathway while preserving the T cell–activating CD47/SIRPγ axis (10). Lastly, Ab-based therapies that target myeloid cells directly may also engage additional surface receptors, such as FcγRs, to further drive myeloid effector functions.

However, targeting SIRPα poses several challenges, including the existence of multiple SIRPα polymorphisms within the human population. The gene encoding SIRPα, *SIRPA*, is highly polymorphic in the IgV domain (21). Although 10 human (hu)SIRPα alleles have been described (21), 3 dominant variants, SIRPα v1, v2, and v8, account for >90% of the alleles found in human populations (22, 23). A further challenge in targeting this family is the existence of other SIRP family members expressed on immune cells, such as SIRPβ1 and SIRPγ, which are highly homologous with SIRPα (4). Therefore, the optimal therapeutic Ab would bind all allelic variants of SIRPα to treat a diverse patient population, while maintaining SIRPα binding specificity (i.e., without engaging SIRPβ and SIRPγ).

In this study, we report on an anti-SIRPα Ab, AL008, that induces internalization and degradation of SIRPα and, concurrently, activates myeloid cells through engaging FcγR2A (CD32A), an activating Fc receptor. Due to its unique epitope, AL008 binds to the major variants of SIRPα without engaging SIRPβ or SIRPγ, a binding specificity needed for broad and potent antagonism of checkpoint activity. Compared to ligand-blocking anti-SIRPα and anti-CD47 Abs, AL008 displays superior potency in inducing macrophage-mediated phagocytosis and T cell activation by dendritic cells. In vivo, AL008 demonstrated single-agent and combination activity in tumor models and showed no evidence of immune cell depletion. The dual mechanism of AL008, which couples the removal of an inhibitory signal (i.e., SIRPα degradation) with immune stimulation (FcγR2A activation), to our knowledge, provides a novel therapeutic strategy for targeting myeloid cells for immune activation.

Materials and Methods

Abs and reagents

AL008 was generated using hybridoma technology by immunizing 17-wk-old NZB/W mice with huSIRPα and CpG-ODN adjuvant. Lymphocytes were isolated from the immunized animals and fused with either SP2/0 or P3X63Ag8 mouse myeloma cells. SIRPα-reactive Abs were screened by binding to SIRPα cell lines or proteins and functional SIRPα Abs identified by phagocytosis assays. A hybridoma clone was identified and humanized by CDR grafting onto a huIgG1 κ backbone containing the N325S and L328F mutations in the CH2 domain to create AL008. In syngeneic tumor studies, a chimeric form of AL008 was produced on a mouse IgG2A Fc backbone to minimize immunogenicity. Anti-mouse programmed death-ligand 1 (PD-L1) (clone 10F.9G2) and corresponding isotype controls, rat IgG2b and mouse IgG2A, were purchased from Bio X Cell. Additional anti-SIRPα Abs (KWAR23, 18D5, 1H9, clone 173) and anti-CD47 Abs (5F9) were produced at Alector based on reported sequences (11, 24, 25). Recombinant huIgG1 N325S/L328F (NSLF), matching the Fc domain sequence of AL008, was used as an isotype control Ab in studies establishing the activity of AL008. An additional isotype control Ab, IgG4, was used alongside recombinant huIgG1 NSLF in assays involving competitor anti-SIRPα and anti-CD47 Abs. When huIgG1 NSLF and IgG4 were each used as isotype controls, only huIgG1 NSLF was shown in the figures. Recombinant anti-CD20 huIgG1 was purchased from InvivoGen.

Binding characterization of AL008

CHO cells expressing human (hu)SIRPα (CHO-huSIRPα) cells at 10^6/ml in FACS buffer (PBS containing 2% FBS) were plated into a 96-well plate. Serial dilutions of unconjugated Abs were incubated with cells for 0.5 h on ice, washed, and stained with anti-human PE-conjugated secondary Ab. Cells were washed twice in cold FACS buffer and analyzed by flow cytometry on a BD FACSCanto (BD Biosciences, San Jose, CA). Data analysis and calculation of mean fluorescence intensity values were performed with FlowJo software (FlowJo, Ashland, OR).

By ELISA, 96-well Immulon HBX plates were coated with Fc-tagged huSIRPα variant 1, variant 2, and variant 8 at 1 μg/ml in PBS overnight at 4°C. Plates were blocked in 5% (w/v) BSA in PBS for 1 h, after which they were washed three times with PBS/0.05% Tween 20 (PBS/T). Abs were added to the plate in a dilution series and were incubated at room temperature for 2 h, after which the unbound Ab was removed by washing with PBS/T. HRP-conjugated anti-human κ L chain secondary Ab (Jackson ImmunoResearch Laboratories) was then added to the wells and incubated for 30 min. Unbound Ab was removed by washing with PBS/T, after which bound Ab was detected using tetramethylbenzidine. The reaction was stopped with 2 N H_2SO_4, after which the plates were read at 450 nm.

Cells

All human tumor cell lines (Raji, Jurkat, MDA-MB-231, and A375) were purchased from American Type Culture Collection (Manassas, VA). Cells were maintained in RPMI 1640 medium supplemented with 10% heat-inactivated HyClone FBS in a humidified chamber of 95% air/5% CO_2 at 37°C.

Fifty-milliliter samples of whole blood collected in EDTA-containing tubes from healthy volunteers were purchased from Blood Centers of the Pacific/Vitalant and shipped at 4°C for next day delivery and cell processing. Blood products were drawn from research donors recruited and consented under the Vitalant research donor protocol using Food and Drug Administration–approved collection methods. Human PBMCs were isolated by Ficoll gradient centrifugation and washed twice in PBS. Leukocyte viability was determined using a Vi-CELL cell viability analyzer (Beckman Coulter) and yielded >95% viable cells. Monocytes were enriched by negative selection using a RosetteSep human monocyte enrichment kit (STEMCELL Technologies) according to the manufacturer's guidelines. T cells were enriched by negative selection using an EasySep human T cell enrichment kit (STEMCELL Technologies) according to the manufacturer's guidelines. Isolated human monocytes were differentiated into macrophages for 7 d using 50 ng/ml M-CSF (PeproTech) in RPMI 1640 medium supplemented with 10% heat-inactivated HyClone FBS and 2 mM GlutaMAX. Isolated human monocytes were differentiated into dendritic cells for 7 d using 20 ng/ml GM-CSF and 20 ng/ml IL-4 (PeproTech) in RPMI 1640 medium supplemented with 10% heat-inactivated FCS.

Internalization of SIRPα and Fcγ receptors

Macrophages were derived by culturing monocytes (Vitalant) in complete growth media supplemented with 50 ng/ml huM-CSF (PeproTech) for 7 d. Cells were plated in 96-well plates at 100,000 cells/ml in RPMI 1640 supplemented with 10% HyClone FBS. AL008 Abs or isotype control Abs were added and cells incubated overnight at 37°C with 5% CO_2. For examining SIRPα cell surface expression, cells were incubated with anti-SIRPα (clone 173) DyLight 650–conjugated Ab for 30 min on ice. For the competition assay, macrophages were preincubated with increasing concentrations of AL008 or other anti-SIRPα Abs, as indicated, at 4°C and subsequently stained with the FACS detection Ab. For the receptor shedding assays, 1×10^5 monocyte-derived macrophages from five donors were pretreated with AL008 or isotype control and then treated with vehicle, PMA (AdipoGen) at 100 ng/ml, or LPS (InvivoGen) at 2.5 μg/ml for 6 h. Cells were pelleted and stained for SIRPα cell surface expression as previously described. The supernatant was collected and levels of soluble SIRPα were determined by ELISA according to the manufacturer's instructions (R&D Systems, catalog no. DY4546-05).

For detecting human FcγR expression, cells were incubated with fluorescently labeled anti-FcγRI (clone 10.1, BioLegend), anti-FcγRIIA (clone IV.3), anti-FcγRIIB (clone 2B6), or anti-FcγRIIIA (clone 3G8). Cells were washed twice in FACS buffer (PBS + 2% FBS) and flow cytometry was performed on a BD FACSCanto. Data were analyzed using FlowJo software (FlowJo, Ashland, OR). Data were calculated as a percent of receptor expression in isotype-treated cells using mean fluorescence intensity values.

Western blot analysis of SIRPα expression

Monocyte-derived macrophages were differentiated from $CD14^+$ monocytes from healthy volunteers as previously described. Five million macrophages were incubated overnight with AL008 or isotype control at 5 μg/ml. Cells were harvested and washed with cold PBS and lysed in cold lysis buffer (*n*-dodecyl-β-maltoside 1%, 50 mM Tris-HCl [pH 8.0], 150 mM NaCl, 1 mM EDTA, 1.5 mM $MgCl_2$, and 10% glycerol plus protease and phosphatase inhibitors). Whole-cell lysates were recovered by pelleting cellular debris and collecting the supernatant fraction. Proteins were resolved by SDS-PAGE, transferred to a polyvinylidene difluoride membrane, and probed with rabbit anti-SIRPα Ab (Cell Signaling Technology, clone D6I3M).

Shotgun mutagenesis epitope mapping

Epitope mapping was performed by shotgun mutagenesis essentially as described previously (26). A huSIRPα v1 protein expression construct (based on UniProt ID: P78324) was subjected to high-throughput alanine scanning

mutagenesis to generate a comprehensive mutation library. In total, 344 mutant clones were generated (covering aa 31–374), sequence confirmed, and arrayed into 384-well plates. The SIRPA mutation library was transfected into HEK-293T cells and assayed in an immunofluorescence FACS assay, in duplicate, for binding by AL008 Fab and other anti-SIRPα Abs. Ab reactivity against each mutant SIRPα clone was calculated relative to wild-type SIRPα protein reactivity by subtracting the signal from mock-transfected controls and normalizing to the signal from wild-type SIRPα-transfected controls. Mutations within clones were identified as critical to the AL008 epitope when they did not support reactivity of the AL008 Fab, but supported reactivity of other SIRPα Abs. This counter-screen strategy facilitates the exclusion of SIRPα mutants that are locally misfolded or have an expression defect.

Phagocytosis assays

Human macrophages (1×10^5) were seeded onto low-attachment 96-well round-bottom plates in complete growth media along with $2.5–4.0 \times 10^5$ Raji, A375 melanoma cells, MDA-MB-231, or Jurkat tumor cells labeled with CFSE dye. In some cases, an Ab-dependent cellular phagocytosis (ADCP) assay was performed by adding 1 μg/ml anti-CD20 Ab. Abs to SIRPα or CD47 were added at a single concentration of 1 μg/ml or at multiple concentrations in dose response. Blocking Abs to FcγR2A (10 μg/ml) and FcγR2B (10 μg/ml) were added in some conditions. After overnight incubation, cells were pelleted and resuspended in FACS buffer containing Fc block. Macrophages were detected by staining cells with anti-CD14 Ab (allophycocyanin) on ice for 15 min. Phagocytosis was measured by analyzing cells with FACSCanto (BD Biosciences, San Jose, CA) and quantifying the percentage of the $CD14^+CFSE^+$ macrophage population. Macrophages treated with human isotype controls served to establish a baseline value for phagocytic activity, and changes in this function with anti-SIRPα or anti-CD20 Ab treatments are presented relative to this baseline value.

Macrophage-mediated tumor cell killing

MDA-MB-231 cells, engineered to stably express luciferase and GFP, were seeded in flat-bottom 96-well plates at a concentration of 1×10^4 cells per well. Tumor cells were cultured alone or with 5×10^4 human monocyte-derived macrophages for 2 d in RPMI 1640 medium supplemented with 10% heat-inactivated HyClone FBS and 20 ng/ml huIL-4 (PeproTech). Cells were treated with 2 μM paclitaxel (PTX), 1 μg/ml AL008, or both. Tumor cell viability was measured by adding an equal volume of ONE-Glo luciferase substrate (Promega) to wells according to the manufacturer's instructions. Luminescence readings were captured on Synergy H1 multi-mode reader (BioTek Instruments).

MLRs

Human dendritic cells were derived by culturing monocytes from healthy donors in RPMI 1640 medium supplemented with 10% heat-inactivated HyClone FBS and 20 ng/ml huGM-CSF huIL-4 (PeproTech) for 7 d in a humidified chamber of 95% air/5% CO_2 at 37°C. T cells from an allogeneic donor were isolated using EasySep Direct Human T Cell Isolation Kit (STEMCELL Technologies, Cambridge, MA). T cells were labeled with CFSE dye to monitor proliferation by dye dilution. Briefly, T cells were washed and suspended in 1× PBS at 10 million cells/ml and stained with 5 μM CFSE (Thermo Fisher Scientific) for 10 min at room temperature shielded from light. Dye conjugation was quenched by washing cells twice with serum-supplemented 1× PBS. Labeled T cells were resuspended in RPMI 1640 medium supplemented with 10% heat-inactivated HyClone FBS at 1 million cells/ml. For one-way MLR, $2–3 \times 10^4$ human dendritic cells were seeded onto 96-well flat-bottom plates in RPMI 1640 medium supplemented with 10% heat-inactivated HyClone FBS and treated with AL008, anti-CD47, or isotype control Abs. Subsequently, 1×10^5 CFSE-labeled allogeneic T cells were added to dendritic cells and incubated in a humidified chamber of 95% air/5% CO_2 at 37°C. As a negative control, CFSE-labeled T cells were cultured alone to establish CFSE intensity of non-divided cells. After 5–6 d, cells where harvested and labeled with anti-CD3 allophycocyanin Abs and analyzed by flow cytometry on a BD FACSCanto (BD Biosciences, San Jose, CA). Total T cells were captured on the allophycocyanin channel and proliferating T cells on the FITC channel. Data analysis and calculation of percent proliferating T cells (ratio of $CD3^+FITC^{low}$ T cells divided by total T cells) was performed with FlowJo software (FlowJo, Ashland, OR). AL008, anti-CD47, and isotype control were all tested at a concentration of 10 μg/ml with isotype control-treated cells to establish baseline T cell activity.

Depletion assay

Human PBMCs from blood of healthy volunteers were isolated by density gradient centrifugation. PBMCs were cultured in RPMI 1640 media supplemented with 10% FBS, 1% penicillin/streptomycin, and 200 ng/ml IL-2, an immunostimulatory cytokine known to enhance cytotoxicity (27). An anti-CD52 huIgG1 Ab, reported to mediate immune cell depletion (28), served as a positive control to validate assay conditions. Cells (500,000) were seeded onto 96-well plates with 20 μg/ml test Abs or isotype control and incubated overnight at 37°C. The following day, cells were processed for flow cytometry analysis and stained for specific lineage markers: CD14 (monocytes), CD3 (T cells), and CD20 (B cells). Counting beads were added to each well and used to quantify the number of cells from each population remaining in culture.

Effect of AL008 in humanized mice

huNOG-EXL mice were purchased from Taconic Biosciences (Germantown, NY) and housed at Alector in positively ventilated polysulfone cages with HEPA-filtered air at a density of up to five mice per cage. Fourteen-week-old female huNOG-EXL mice ($n = 19$) engrafted with $huCD34^+$ hematopoietic stem cells derived from one healthy donor were inoculated with A375 melanoma cells s.c. in the flank region at a density of 3 million cells per mouse with Matrigel (Corning). When tumors reached an average volume of 200–400 mm^3, mice received i.p. injections of 10 mg/kg huIgG1 NSLF or AL008 on days 1 and 4. Splenic and tumor tissues were mechanically dissociated followed by 1-h enzymatic dissociation of tumor tissues using a human tumor dissociation kit from Miltenyi Biotec. Sample material was passed through a 70-μm filter to obtain single-cell suspensions. Peripheral blood was treated with ammonium-chloride-potassium lysis buffer to lyse RBCs and washed with PBS. Cells were resuspended in FACS buffer with FcγR-blocking Abs and maintained on ice to preserve viability and marker expression. Cells were stained with anti-CD45, CD11b, anti-CD14, anti-CD163, anti-HLA-DR, anti-CD86, and anti-SIRPα Abs to delineate myeloid subpopulations. Anti-SIRPα Ab used in this study does not compete with AL008 binding and can be used to detect SIRPα expression in the presence of AL008 binding.

The effect of AL008 on tumor growth was assessed in humanized NSG (NOD.Cg-*Prkdc*^{scid} *Il2rg*^{tm1Wjl}/SzJ) mice purchased from and housed by The Jackson Laboratory. Female $huCD34^+$ NSG mice ($n = 22$) reconstituted with $huCD34^+$ hematopoietic stem cells from two different donors were implanted orthotopically in the mammary fat pad with MDA-MB-231 cells at 5×10^6 cells, resuspended in a 1:1 mixture of PBS and Matrigel. When tumor volumes reached ~60–100 mm^3, mice were randomized into treatment groups based on tumor volume, $CD34^+$ donor, and tumor growth rate. All groups allocated seven to eight mice to maintain equivalent average tumor volume. Beginning on the following day (day 0), mice were dosed with 40 mg/kg AL008 or isotype control every 4 d for 8 doses. Mice administered pembrolizumab received 10 mg/kg anti–programmed death-1 (PD-1) Ab for the first dose and 5 mg/kg for the next 7 doses to limit the significant weight loss often observed in this model.

Syngeneic tumor models

In MC38 cells, the mouse CD47 gene was knocked out through CRISPR-mediated engineering. Briefly, Cas9/guide RNA (gRNA) complexes were introduced into the MC38 target cells. Cas9/gRNA-mediated indel formation at the targeted region (exon 2 of mouse CD47) resulted in frameshift and/or premature stop, thus knocking out expression of the mouse CD47 gene. After transfecting gRNA and Cas9, single cell–derived clones were screened by sequencing, and homozygous clones containing the desired mutation were expanded. The MC38–mouse CD47 knockout cells were then transduced with a lentivirus containing the huCD47 gene insert. MC38-$huCD47^+$ cells were selected with puromycin and expanded.

huSIRPA/huCD47 mice were implanted with MC38-$huCD47^+$ tumor cells and received two doses of 3 mg/kg AL008, 10 mg/kg AL008, or isotype control (mouse IgG2A) Ab. On days 1, 4, and 8 postdose, tumors were harvested and dissociated, and myeloid cells were stained for huSIRPα using an anti-SIRPα clone that does not compete with AL008 binding. Tumor-infiltrating myeloid cell populations were analyzed for changes in cell surface levels of SIRPα.

Alector generated C57BL6/J transgenic (Tg) mice by inserting BAC clones expressing huSIRPα (BACRP11-636L228) and huCD47 genes (BACRP11-671F8). Eight- to 12-wk-old female huSIRPA/huCD47 BAC Tg mice housed at Charles River Laboratories were implanted with MC38-$huCD47^+$ tumor cells s.c. in the flank region at a density of 100,000 cells per mouse. When tumors reached an average volume of ~100 mm^3, mice were randomized into treatment groups, and dosing was initiated on day 1. All groups were allocated 9–10 mice to maintain equivalent average tumor volume at treatment initiation. Mice received i.p. injections of isotype control or AL008 with or without anti–PD-L1 combination twice per week for 3 wk. Tumors were also measured twice per week with calipers; volumes were calculated according to the following formula: $0.52(\text{length} \times \text{width}^2)$.

Statistical analysis

Statistical analysis was performed using GraphPad Prism 8.0. A two-tailed *t* test was used for comparisons between two groups. A one-way ANOVA followed by the Holm–Sidak method of multiple comparisons was used for comparisons of more than two groups. A p value of ≤ 0.05 was considered significant.

Study approval

All in-house animal studies were reviewed by, approved by, and performed in compliance with Alector's Institutional Animal Care and Use Committee protocols. Outsourced studies were conducted in accordance with the applicable Charles River Laboratories standard operating procedures, which approved these studies.

Results

AL008 binds to major variants of SIRPα without engaging SIRPβ or SIRPγ

AL008 bound the major allelic variants of huSIRPα (variants 1, 2, and 8; Fig. 1A, Supplemental Fig. 1A) without cross-reacting to human SIRPβ1 or SIRPγ (Fig. 1A, 1B). Affinity measurements of AL008 for SIRPα v1 ranged between 3 and 12 nM (Fig. 1C). In contrast, other anti-SIRPα Abs either displayed broad cross-reactivity to SIRPβ (KWAR23, 18D5; Supplemental Fig. 1B) and/or SIRPγ (KWAR23; Supplemental Fig. 1B) (12) or bound only a subset of SIRPα alleles (18D5; Supplemental Fig. 1A). AL008 also binds to cynomolgus monkey SIRPα, enabling the use of this nonhuman primate species for preclinical toxicity studies (Supplemental Fig. 1C). Epitope mapping through alanine-scanning mutagenesis revealed that AL008 recognizes a SIRPα-specific sequence (R282, Q284, G337) located within the membrane-proximal IgC2 domain, which is conserved among SIRPα variants but not in SIRPβ1 or SIRPγ (Fig. 1D). This epitope mapping is consistent with the binding specificity observed with AL008 (Supplemental Fig. 2A, 2B).

Because the CD47-binding site maps to the IgV domain of SIRPα, the ability of AL008 to impede ligand binding was assessed in a cell-based assay in which fluorescently labeled huCD47 tetramers stained a mouse cell line overexpressing huSIRPα (BWZ-SIRPα). Consistent with the epitope mapping data, AL008 did not competitively block CD47 binding in BWZ-huSIRPα cells stained with the tetramer at 4°C for 30 min (Fig. 2A). In contrast, KWAR23 (anti-pan SIRPα) and 18D5 (anti-SIRPα v1) competitively blocked CD47 binding in a dose-dependent manner (Fig. 2A), as previously reported (10, 29). AL008 demonstrated an ability to internalize SIRPα in human monocyte-derived macrophages after overnight incubation at 37°C (Fig. 2B). A time course analysis showed that SIRPα internalization was observed at 1 h after incubation and maximum internalization was achieved by 6 h (data not shown). Ligand-blocking Abs (KWAR23, 18D5, 1H9) failed to internalize SIRPα on macrophages (Fig. 2B). Importantly, reduction of cell surface SIRPα is not a consequence of AL008 interfering with staining by the anti-SIRPα FACS detection Ab. In a competition assay, neither AL008 nor ligand-blocking anti-SIRPα Abs prevented the FACS Ab from recognizing SIRPα on macrophages (Fig. 2B).

Previous reports indicate that SIRPα is proteolytically cleaved from the cell surface in response to proinflammatory stimuli, such as LPS and PMA (30). To determine whether AL008-mediated reduction in surface SIRPα is due to internalization or shedding of the receptor,

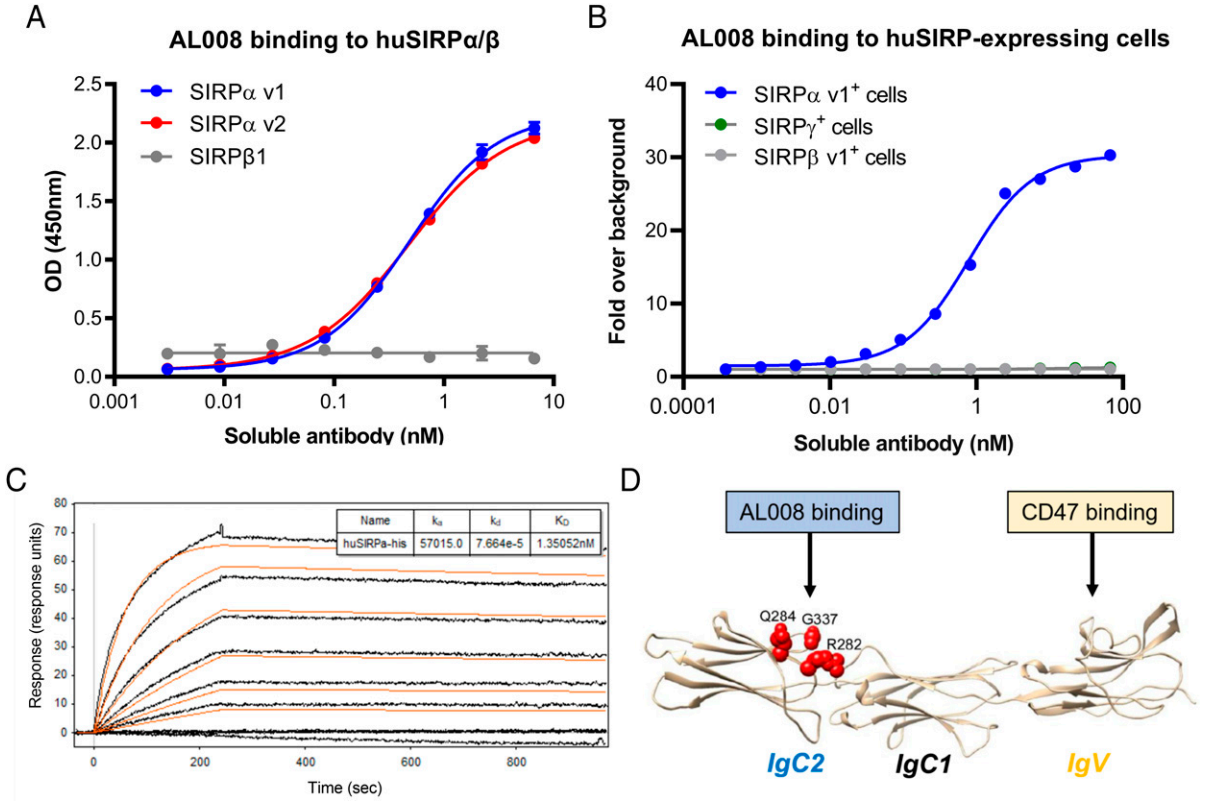

FIGURE 1. AL008 is a pan-SIRPα binding Ab that does not bind SIRPβ1 or SIRPγ. (**A**) Titration curves of AL008 binding to human SIRP proteins by ELISA are shown. (**B**) AL008 binding to human SIRP Ags overexpressed on cell lines is shown. AL008 was detected with a fluorescent anti-human IgG Fc secondary Ab. The data series for SIRPγ$^+$ cells (green lines) and SIRPβ v1$^+$ cells (gray lines) are superimposable. (**C**) Surface plasmon resonance was performed with a Biacore T200 system at 25°C to determine the affinity of AL008 for human SIRPα v1. Anti-human IgG was amine-coupled to a Biacore CM5 sensor chip to capture AL008, and soluble His-tagged SIRPα v1 diluted in HBS-EP$^+$ with 1 mg/ml BSA was injected in a concentration series ranging from 0.3215 to 40 nM. The data were analyzed using a 1:1 binding model, and the reported on- and off-rates are representative of three independent experiments. (**D**) Alanine scanning mutagenesis defined three residues (red spheres) in the IgC2 domain of human SIRPα critical for Ag binding by AL008.

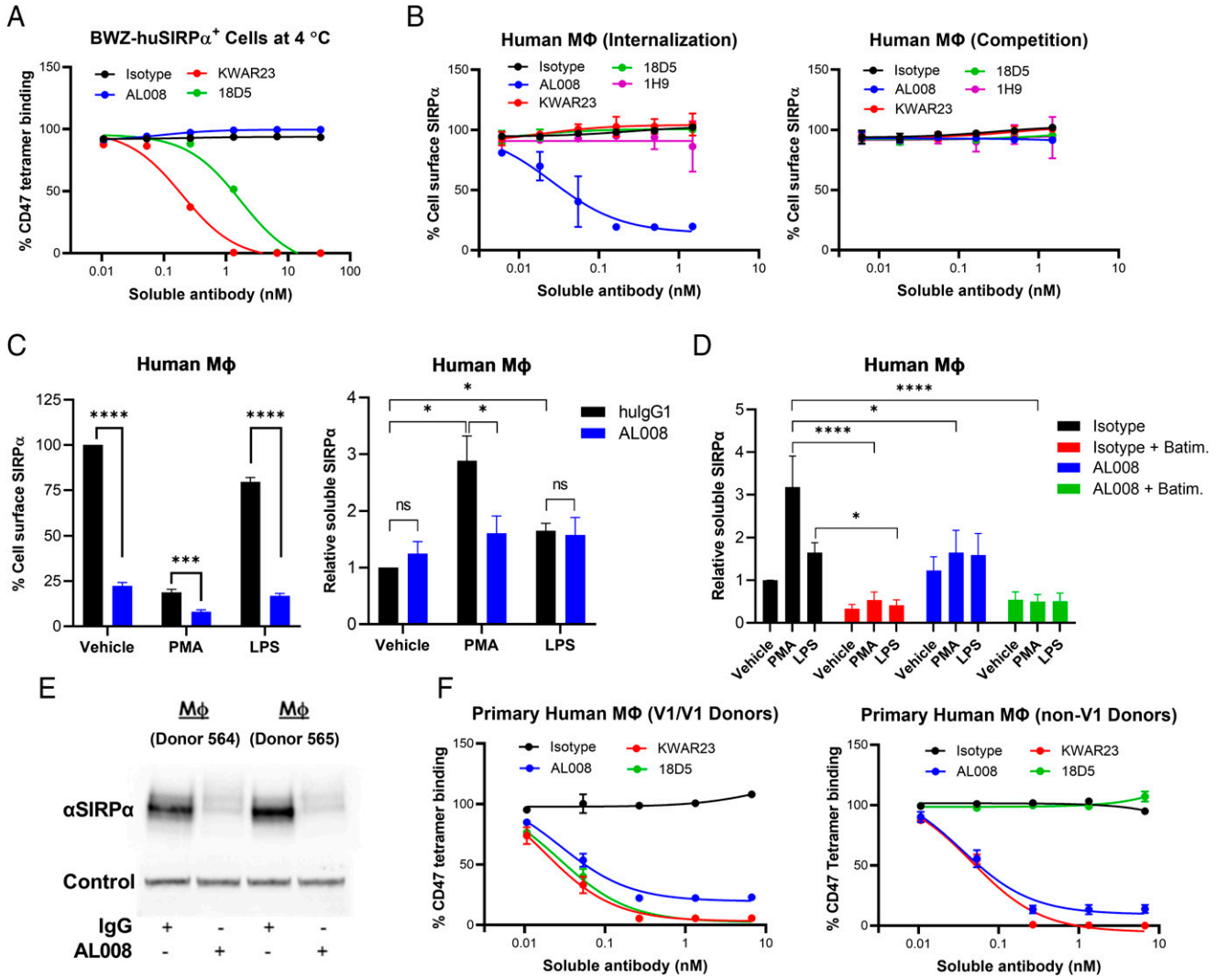

FIGURE 2. AL008 induces the internalization and degradation of SIRPα on human macrophages. (**A**) BWZ-huSIRPα overexpressing cells were incubated in the presence of AL008 or with CD47-blocking anti-SIRPα Abs (i.e., KWAR23, 18D5), followed by incubation with allophycocyanin-labeled human CD47 tetramers. The percentage of CD47 tetramer binding was measured and normalized to Ab control condition. (**B**) A receptor internalization assay was performed on monocyte-derived macrophages treated overnight with increasing concentrations of the indicated Abs. A competition assay was performed under similar conditions, except macrophages were treated with test Abs at 4°C for 30 min. Cell surface SIRPα was detected by flow cytometry with a fluorescent anti-human SIRPα Ab that does not compete with test Ab binding. Relative expression levels of SIRPα were normalized to the isotype-treated cells. Data are means ± SD. (**C**) Macrophages from five donors were pretreated with AL008 and then treated with vehicle, PMA, or LPS (left panel). The supernatant was collected and levels of soluble SIRPα were determined (right panel). Data are means ± SEM. (**D**) The protease inhibitor batimastat prevents the PMA- and LPS-induced increase in soluble SIRPα. Data are means ± SEM. Soluble SIRPα values from isotype-treated vehicle control cells were normalized for each donor. (**E**) Western blot analysis reveals AL008-mediated degradation of SIRPα. (**F**) Macrophages that are homozygous for the v1 variant of SIRPα (left) or are expressing a non-v1 variant of SIRPα (right) were treated overnight with increasing concentrations of AL008, CD47-blocking anti-SIRPα Abs, or isotype control. Cells were stained with allophycocyanin-labeled human CD47 tetramers. Relative CD47 binding was normalized to isotype-treated cells. Isotype control shown is human IgG1 NSLF. Data are means ± SD. For (C) and (D), a one-way ANOVA was performed followed by Holm–Sidak's method of multiple comparisons. $*p < 0.05$, $***p < 0.001$, $****p < 0.0001$. ns, not significant.

the concentration of soluble SIRPα was measured in the media fraction following stimulation of human macrophages with AL008, LPS, or PMA. AL008 reduced cell surface SIRPα compared with isotype control, as did the immune activators PMA and LPS (Fig. 2C, left panel), as previously reported (30). AL008 pretreatment enhanced the PMA- and LPS-induced reduction in cell surface SIRPα (Fig. 2C, left panel). In an accompanying assay, AL008 pretreatment did not increase soluble SIRPα in the supernatant compared with isotype control. Conversely, in isotype pretreated cells, PMA and LPS significantly increased soluble SIRPα compared with vehicle (Fig. 2C, right panel), indicating that AL008 does not induce shedding compared with PMA and LPS. Notably, AL008 pretreatment reduced the generation of soluble SIRPα from PMA-treated macrophages, consistent with AL008 reducing surface SIRPα available for PMA-induced shedding (Fig. 2C, right panel). Furthermore, batimastat, a broad-spectrum protease inhibitor, significantly blocked the PMA- and LPS-induced increase in soluble SIRPα (Fig. 2D), confirming that soluble SIRPα results from protease-induced receptor shedding. Finally, we observed that Ab-mediated SIRPα internalization by AL008 resulted in receptor degradation in macrophages as measured by Western blots of total SIRPα in cell lysates (Fig. 2E), establishing an additional mechanism for antagonizing SIRPα.

Repeating the CD47-binding assay with human monocyte-derived macrophages treated with either AL008 or ligand-blocking Abs overnight (Fig. 2F) demonstrated reduced binding of CD47 tetramers compared with isotype control. AL008 inhibited CD47 binding to

macrophages regardless of the SIRPα allelic variant expressed by donors (Fig. 2F) and in all donors tested (data not shown). This pan-allelic reactivity contrasts with anti-SIRPα v1-specific Ab (18D5), which only blocks CD47 binding to macrophages homozygous for SIRPα variant 1 (9). Taken together, these data demonstrate that AL008 is a pan-allelic, SIRPα-specific Ab that antagonizes ligand binding through a noncompetitive mechanism resulting in SIRPα internalization and degradation.

AL008 enhances macrophage phagocytosis

The functional activity of AL008 was assessed in vitro using human macrophage-based phagocytosis assays, a function that is reported to be highly influenced by CD47–SIRPα interactions. $CD14^+$ macrophages were cocultured with CFSE-labeled cancer cells in the presence of isotype control, AL008 mAbs, or cytochalasin D, an inhibitor of phagocytosis. The percentage of phagocytosis was determined by the percentage of $CFSE^+$ cells within the CD14 allophycocyanin$^+$ macrophage cell gate. Population gates were established by monocultures of $CFSE^+$ cancer cells and $CD14^+$ human macrophages (Fig. 3A). In an ADCP assay, macrophages treated with AL008 significantly enhanced anti-CD20–mediated phagocytosis of Raji cells compared with isotype control across six donors tested (Fig. 3B). AL008-treated human monocyte-derived macrophages exhibited a statistically significant increase of ~50% in ADCP activity relative to control-treated macrophages. In contrast, the ligand-blocking SIRPα Ab, 18D5, demonstrated significantly less ADCP activity compared with AL008, and KWAR23 trended in the same direction (Fig. 3B).

To assess the ability of AL008 to increase macrophage-mediated phagocytosis of hematopoietic and solid tumor cell lines in the absence of an opsonization agent, human monocyte-derived macrophages from six to eight different healthy blood donors were coincubated with fluorescently labeled Raji, MDA-MB-231 (breast cancer), A375 (melanoma), or Jurkat (lymphoma) human tumor cell lines. AL008-treated human monocyte-derived macrophages significantly increased phagocytosis of Raji, MDA-MB-231, A375, and Jurkat cells by 100, 80, 74, and 83%, respectively, compared with control-treated macrophages (Fig. 3B, 3C). As was observed with the ADCP assay, ligand-blocking anti-SIRPα Abs (KWAR, 18D5, 1H9) displayed significantly reduced induction of phagocytosis compared with AL008 across all tumor cell lines tested in the absence of opsonization agent (Fig. 3C). These data demonstrate the single-agent ability of AL008 to stimulate phagocytic activity in both hematopoietic and solid tumor cell lines.

In addition to tumor cell phagocytosis, AL008 was assessed for its ability to stimulate macrophage-mediated tumor cell killing in combination with the anticancer cytotoxic agent PTX in MDA-MB-231 cells. Both AL008 and PTX as single agents reduced viable tumor cells when cultured in the presence of macrophages, as reflected by a decrease in luminescence. In the presence of macrophages, AL008 + PTX treatment reduced viable tumor cells significantly more than PTX treatment alone (Supplemental Fig. 3). These results further demonstrate that AL008 stimulates macrophage-mediated tumor cell clearance in vitro.

AL008 promotes T cell function and does not mediate depletion

Targeting the CD47–SIRPγ interaction through anti-CD47 mAbs or an anti-SIRPγ has been shown to inhibit T cell proliferation (17, 31, 32). Because AL008 does not interfere with the CD47–SIRPγ interaction, we conducted experiments to investigate the effect of AL008 on T cell function. We evaluated the effect in an MLR assay of human monocyte-derived dendritic cells cocultured with allogeneic T cells labeled with CFSE dye. AL008 increased T cell proliferation

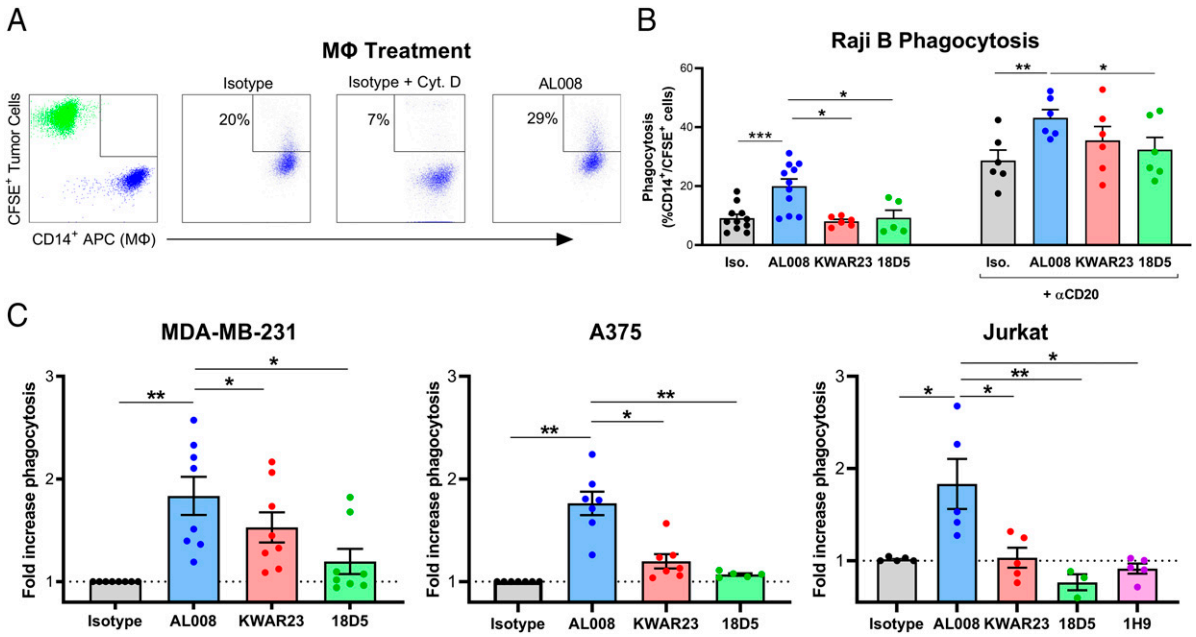

FIGURE 3. AL008 enhances the phagocytosis of tumor cells by macrophages. (**A**) FACS plots showing the gating strategy for measuring phagocytosis of $CFSE^+$ Raji cells and CD14-allophycocyanin$^+$ macrophages. $CFSE^+$ Raji cells were run in the upper left quadrant (green), and CD14-allophycocyanin$^+$ macrophages were run in the lower right quadrant (blue). Phagocytosis is shown in the upper right quadrant. (**B**) AL008 increased Ab-dependent cellular phagocytosis (ADCP) of anti-CD20 opsonized Raji B cells (right) and induced phagocytosis of Raji cells in the absence of an opsonization agent (left). Human monocyte-derived macrophages were treated with isotype control, AL008, or SIRPα-blocking Abs and cocultured with fluorescently labeled tumor cells. Raji cells were opsonized with anti-CD20 Ab as indicated. ADCP of Raji cells was measured by flow cytometry gating on the percentage of $CD14^+/CFSE^+$ macrophages. (**C**) AL008 promotes the phagocytosis of solid tumor and lymphoma cell lines by macrophages in the absence of opsonizing antitumor Abs. Macrophages were treated as previously described and cocultured with CFSE-labeled tumor cell lines. Phagocytosis of tumor cells was measured by flow cytometry gating on the percentage of $CD14^+/CFSE^+$ macrophages. Results were normalized to the isotype-treated cells. Each symbol represents macrophages from a different human donor. Paired Student *t* tests were performed. $*p < 0.05$, $**p < 0.01$, $***p < 0.001$.

compared with isotype control, whereas anti-CD47–blocking Ab (5F9) significantly reduced T cell proliferation (Fig. 4A). These effects were observed across multiple distinct donors, with AL008 significantly enhancing T cell proliferation by ~30% in comparison with isotype control or by 68% in comparison with anti-CD47 Ab (Fig. 4B). These data further demonstrate an advantage of targeting SIRPα compared with CD47. In contrast to ligand-blocking anti-SIRPα Abs, such as 18D5 and 1H9, which were reported to have no effect on T cell function in an allogeneic MLR (10, 12), AL008 appears to promote dendritic cell–mediated T cell proliferation.

As SIRPα has a more restricted expression pattern compared with CD47, we also compared the ability of AL008 and anti-CD47 to mediate PBMC depletion in an in vitro assay using multiple healthy donors. The Fc domain of AL008 contains the NSLF mutations on a huIgG1 backbone to abrogate binding to FcγR3 and enhance binding to FcγR2A relative to wild-type huIgG1 (33). In this Ab-dependent cellular cytotoxicity (ADCC) assay, AL008 did not induce depletion of any immune cell type, including monocytes, which express high levels of SIRPα, whereas anti-CD47 significantly reduced monocytes, T cells, and B cells (Fig. 4C, B cell data not shown). In addition, we tested whether AL008 would mediate depletion of T cells by macrophages in an ADCP setting in the presence of an anti–PD-1 or anti–PD-L1 Ab. As in the ADCC assay, AL008 did not deplete $CD4^+$ T cells under these conditions (Fig. 4D). Taken together, these data highlight a potential of AL008 to enhance T cell function without mediating cell depletion, which stands in contrast to anti-CD47 Abs.

AL008 function requires FcγR2A activation

In several assays, AL008 exhibited greater potency in augmenting macrophage phagocytosis of tumor cells than ligand-blocking anti-SIRPα Abs, suggesting that additional mechanisms may be involved in AL008 function beyond inhibition of ligand binding. In addition to inducing SIRPα degradation from the cell surface, we hypothesized that AL008 may also engage FcγRs to stimulate macrophage activity. To assess the role of FcγRs, an AL008 variant, AL008-LALAPS, was engineered with a series of Fc mutations (L234A, L235A, P331S) known to abrogate FcγR interaction (34, 35). Mutating the Fc domain did not alter Ag recognition (Supplemental Fig. 4A). Ab-mediated SIRPα internalization was diminished in AL008-LALAPS–treated macrophages by ~2-fold relative to AL008-treated macrophages (Fig. 5A). Subsequently, the requirement for FcγR engagement by AL008 was assessed in an ADCP assay as previously described. As shown in Fig. 5B, human macrophages treated with AL008 increased phagocytosis of anti-CD20–coated Raji cells relative to isotype control-treated macrophages, whereas AL008-LALAPS failed to increase macrophage-mediated ADCP of Raji cells. Taken together, the results from receptor downregulation and tumor cell phagocytosis assays establish a necessary role for FcγRs in AL008 activity.

Macrophages express a broad repertoire of activating and inhibitory FcγRs on their surface. Previous studies show that Fc-mediated interaction with FcγRs leads to internalization of FcγRs and activation of downstream effector responses (36–38). FcγR2A is highly expressed on macrophages and is reported to internalize upon engagement with IgG Abs, whereas FcγR2B is an inhibitory FcγR (39, 40). To determine which specific FcγR was required for AL008 function, changes in FcγR expression levels were evaluated by flow cytometry

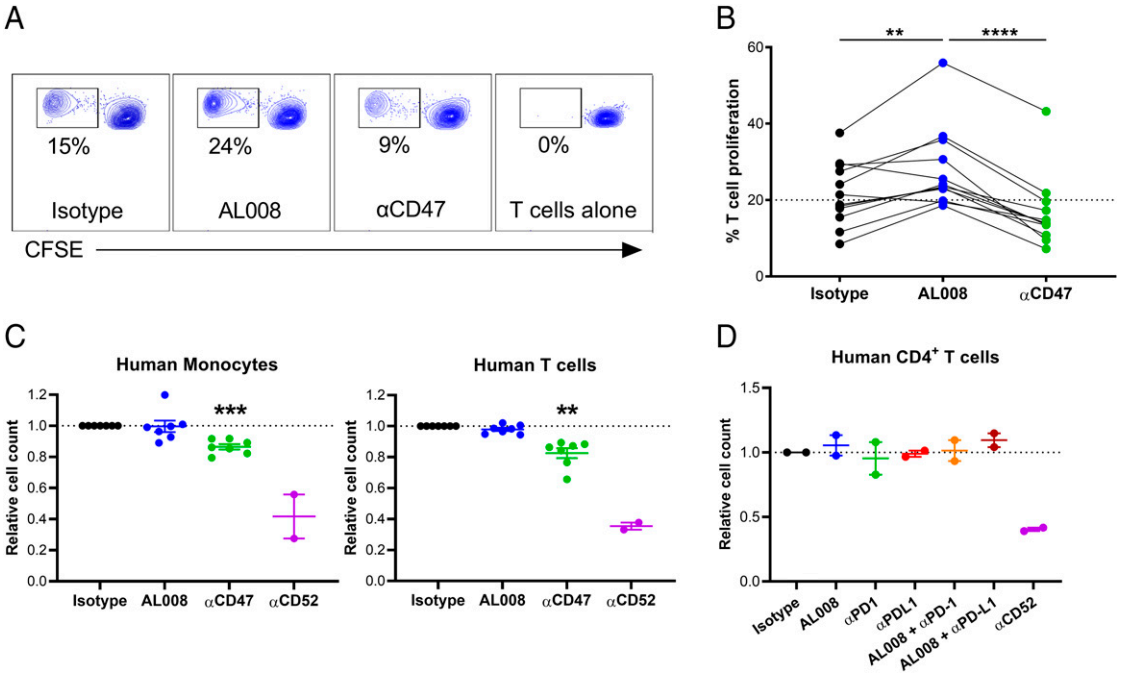

FIGURE 4. AL008 promotes T cell function and shows no evidence of depletion. (**A**) Human monocyte-derived dendritic cells were treated with 10 μg/ml AL008, anti-CD47, or isotype control and cocultured with CFSE-labeled allogeneic $CD3^+$ T cells. Proliferating T cells were measured 6 d later by flow cytometry gating on CFSE-low $CD3^+$ T cells. (**B**) Ten distinct healthy donors were tested in the conditions described in (A). Each symbol represents a different dendritic cell–T cell reaction. A paired Student *t* test was performed. $^{**}p < 0.01$, $^{****}p < 0.0001$. The dashed line represents the median value of isotype-treated cells. (**C**) An ADCC assay was performed using PBMCs from two to six healthy donors. PBMCs were incubated with 200 ng/ml IL-2 overnight, then cells were harvested and incubated with 20 μg/ml AL008, anti-CD47 IgG4, anti-CD52 IgG1, or isotype control for overnight. The remaining cells were stained for monocytes (CD14; left panel), T cells (CD3; right panel), and B cells (CD20; data not shown) and cell counts obtained. For each donor, cell counts were normalized to the isotype control condition. (**D**) An ADCP assay was established using monocyte-derived macrophages, as previously described. Combinations of AL008 with anti–PD-1 and anti–PD-L1 were tested. For (C) and (D), a paired Student *t* test was done. $^{**}p < 0.01$, $^{***}p < 0.001$.

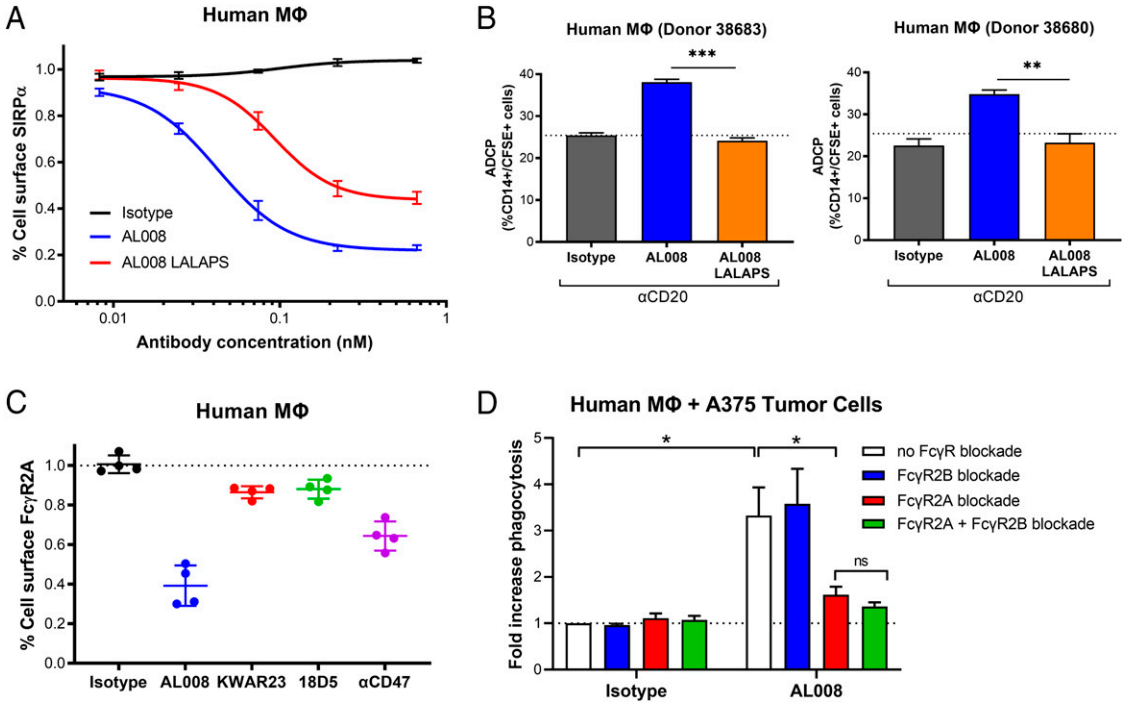

FIGURE 5. AL008 activity depends on FcγR engagement. (**A**) Human monocyte-derived macrophages were treated overnight with increasing concentrations of AL008, AL008-LALAPS, or control Ab. Cell surface SIRPα was detected by flow cytometry with a fluorescent anti-human SIRPα Ab, as previously described. Relative expression levels of SIRPα were normalized to the isotype-treated cells. Graph depicts aggregated data from six different human donors; average ± SEM is shown. (**B**) Macrophages from two separate donors (donor 38683, left panel; donor 38680, right panel) were treated as previously described and cocultured with CFSE-labeled Raji cells opsonized with anti-CD20. ADCP of Raji cells was measured by flow cytometry gating on the percentage of $CD14^+/CFSE^+$ macrophages. A two-tailed *t* test was used to determine the *p* values. $^{**}p < 0.01$, $^{***}p < 0.001$. (**C**) Cell surface FcγR2A was detected by flow cytometry with a fluorescent anti-human FcγR2A Ab (clone IV.3). Relative expression level of FcγR2A was normalized to the control-treated cells. Each symbol represents macrophages from a different human donor. (**D**) Human macrophages were preincubated with blocking Abs against FcγR2A (clone IV.3) or FcγR2B (clone 2B6) either alone or in combination. Subsequently, macrophages were treated with isotype control or AL008 and cocultured with CFSE-labeled tumor cell lines. Phagocytosis of tumor cells was measured by flow cytometry gating on the percent of $CD14^+/CFSE^+$ macrophages. Results were normalized to the isotype-treated cells. Graph depicts aggregated data from four different human donors; average ± SEM is shown. A two-tailed *t* test was used to determine the *p* values. $^{*}p < 0.05$.

on AL008-treated human macrophages. As observed across four donors, overnight treatment with AL008 at 37°C led to the greatest internalization of FcγR2A (~60% relative to IgG; Fig. 5C) with less internalization observed for FcγR2B (~40% relative to IgG) (Supplemental Fig. 4B). As AL008 does not bind to FcγR3A, expression levels of FcγR3A remained constant (Supplemental Fig. 4B). An increase in FcγR1 expression was noted with AL008 (Supplemental Fig. 4B), potentially due to macrophage activation (41). Neither ligand-blocking anti-SIRPα Ab altered the expression of any of these FcRs, again demonstrating a unique feature of AL008 compared with other SIRPα Abs.

To verify the functional role of FcγR2A or FcγR2B, the effect of AL008 on macrophage-mediated phagocytosis of tumor cells was assessed in the presence of blocking Abs specific for each receptor. In the absence of FcγR blockade, AL008 demonstrated an average 3-fold increase in phagocytosis of A375 tumor cells relative to isotype control-treated macrophages averaged among four different healthy donors (Fig. 5D). Blocking Abs against FcγR2A significantly reduced the effect of AL008 on macrophage engulfment of tumor cells, whereas blocking FcγR2B had no significant effect. Simultaneous blockade FcγR2A and FcγR2B did not significantly reduce AL008 function beyond FcγR2A blockade alone. These results support the view that, concurrent with inducing SIRPα internalization and degradation, AL008 engages FcγR2A to stimulate macrophage phagocytic activity.

Effects of AL008 on human TAMs in vivo

A humanized immune system mouse model consisting of NOG-EXL mice reconstituted with human stem cells was used to assess AL008-mediated changes of human TAMs in an in vivo setting. Humanized mice were implanted with A375 tumor cells and randomized into isotype control or AL008 treatment groups. Blood, spleen, and tumor tissue were harvested 24 h after administration of two doses of Ab (Fig. 6A). Myeloid cells from each compartment were analyzed for changes in surface markers consistent with AL008-mediated cellular activation. Monocytes were gated on human $CD45^+CD11b^+CD14^+$ cells present in single-cell suspensions. AL008 reduced cell surface SIRPα expression on blood monocytes by 60% and on splenic monocytes by 70% relative to isotype control (Fig. 6B). Next, we examined the effect of AL008 on tumor macrophages. Tumors were dissociated through enzymatic digestion into single-cell suspensions, and human TAMs were gated on $CD45^+CD11b^+CD14^{hi}CD16^{hi}$ cells (Fig. 6C). As observed with peripheral blood or splenic monocytes, TAMs from AL008-treated animals demonstrated a 70% decrease in surface SIRPα levels relative to isotype-treated animals. These results show that AL008 induced SIRPα internalization in the tumor microenvironment. TAMs were also assessed for changes in surface markers indicative of macrophage activation. TAMs from animals administered AL008 increased expression of M1 markers HLA-DR and CD86 by 112 and 36%, respectively, relative to isotype-treated animals (Fig. 6C). In contrast, expression of the M2 marker, CD163, was not statistically significant between treatment groups (data not shown).

Lastly, the effect of AL008 on tumor growth was assessed in humanized mice implanted with MDA-MB-231 tumors. When tumor volumes reached ~60–100 mm^3, mice were randomized into treatment groups based on tumor volume, $CD34^+$ donor, and tumor growth rate; dosing was initiated the following day (day 0). Compared

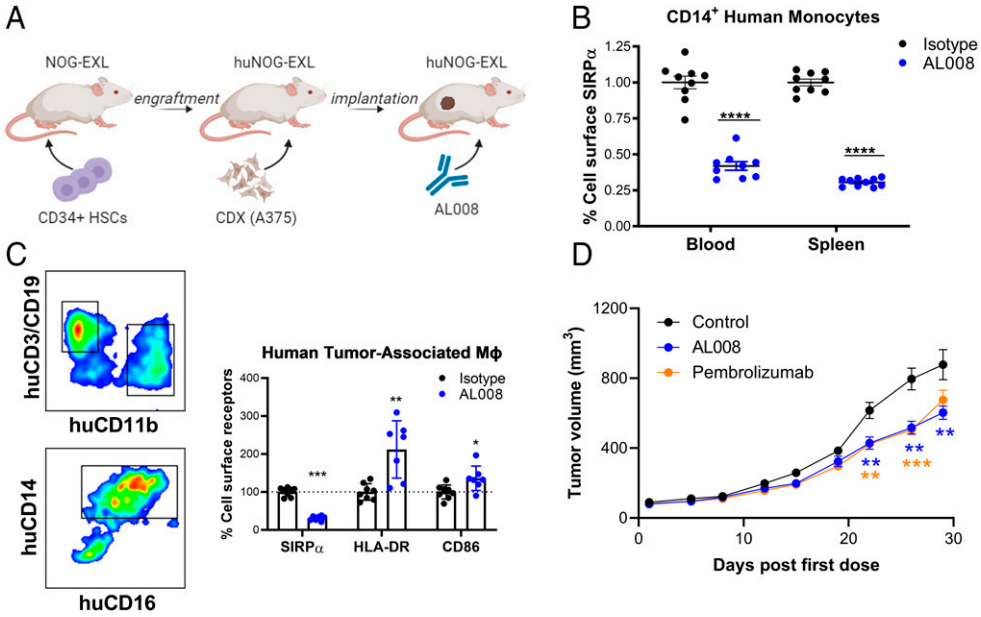

FIGURE 6. Effect of AL008 on human tumor-associated macrophages in a humanized mouse model. (**A**) Immune-deficient NOG-EXL mice were engrafted with human $CD34^+$ hematopoietic stem cells (HSCs) for stable reconstitution of human immune cell lineages. Mice were then implanted s.c. with 3 million cells of A375. When tumors reached a volume of 200–400 mm^3, mice received two doses of AL008 or isotype control 3 d apart. Twenty-four hours after the last dose, blood, spleen, and tumor tissues were harvested and processed for analysis by flow cytometry. (**B**) AL008 internalizes SIRPα on peripheral myeloid cells. Human monocytes from blood and spleen samples were gated on human $CD45^+CD11b^+CD14^+CD16^-$ cells. Cell surface SIRPα was detected by flow cytometry with a fluorescent anti-human SIRPα Ab, as previously described. Relative expression levels of SIRPα were normalized to the isotype-treated animals. Each symbol represents a different animal in the group. $^{****}p < 0.0001$. (**C**) AL008 internalizes SIRPα and increases M1 markers on human tumor-associated macrophages. Macrophages were gated on human $CD45^+CD11b^+CD14^+CD16^+$ cells. A representative gating scheme is shown. Cell surface SIRPα, HLA-DR, and CD86 were detected by flow cytometry. Relative expression levels of the indicated receptor were normalized to the isotype-treated animals. Each symbol represents a different animal in the group. (**D**) Humanized mice implanted with MDA-MB-231 tumors were administered isotype ($n = 7$), AL008 ($n = 8$), or the anti–PD-1 Ab pembrolizumab ($n = 7$). AL008 inhibited tumor growth in a similar manner to pembrolizumab. In (B)–(D), unpaired Student *t* tests were performed. $^*p < 0.05$, $^{**}p < 0.01$, $^{***}p < 0.001$, $^{****}p < 0.0001$ for treatment versus isotype murine IgG1 at a given time point.

to mice dosed with the isotype control Ab, AL008 inhibited tumor growth by 38% (Fig. 6D), analogous to the anti–PD-1 Ab, pembrolizumab (tumor growth inhibition = 34%, Fig. 6D). Thus, the results obtained in humanized immune system mouse models support the view that AL008 mediates internalization of SIRPα and increases M1 markers associated with an antitumoral phenotype.

AL008 delays tumor growth in MC38 syngeneic tumor model

As AL008 does not bind to murine SIRPα, we generated huSIRPα/huCD47 Tg mice to enable testing AL008 in syngeneic tumor models in combination with T cell checkpoint blockade. In these Tg mice, expression of huSIRPα was as anticipated, with expression observed on mouse monocytes, macrophages, and neutrophils, and no expression on lymphocytes (Fig. 7A, data not shown). Human CD47 was expressed on all cells (Fig. 7A, data not shown). In addition, MC38 cells were engineered to replace the murine CD47 gene with huCD47 (MC38-huCD47$^+$), which directs immune suppression through huSIRPα (Fig. 7B). As these mice still express mouse SIRPα and mouse CD47, the presence of the endogenous mouse SIRPα–CD47 pathway likely overlaps in function with the human SIRPα–CD47 pathway, thus limiting the potency of AL008 in these Tg mice.

To confirm activity of AL008 in these huSIRPα/huCD47 Tg mice, we assessed the effect of AL008 on SIRPα expression after in vivo administration to tumor-bearing mice. All AL008-treated animals decreased cell surface huSIRPα expression relative to isotype-treated animals, with a range of 70–80% reduction of surface SIRPα observed (Fig. 7C). Recovery of SIRPα expression followed a dose-dependent pattern with animals receiving 3 and 10 mg/kg AL008 returning to baseline expression levels at 4 and 8 d postdose, respectively. No depletion of myeloid cells or any immune cell population was observed (data not shown). Based on cell surface levels of huSIRPα, a dosing regimen of 10 mg/kg AL008 twice a week was chosen as the dose to continue testing AL008 in the MC38 model.

In efficacy studies, Tg mice were implanted with MC38-huCD47$^+$ cells and randomized to an average tumor volume of 100 mm^3 before initiation of treatment. AL008 or an anti-pan SIRP benchmark Ab (KWAR23) that competitively blocks the interaction with huCD47 was tested in combination with a suboptimal dose of anti–PD-L1 Ab. Anti–PD-L1 Ab monotherapy failed to inhibit tumor growth relative to isotype control. AL008 monotherapy also failed to inhibit tumor growth, likely due to the expression of both mouse and human SIRPα–CD47 pathways in this Tg mouse model (Fig. 7D). However, the combination of anti–PD-L1 with AL008 reduced tumor growth by 41% compared with anti-PD-L1–treated animals, and by 47% compared with isotype-treated animals averaged across both studies shown. In contrast, the combination of anti–PD-L1 with anti-pan SIRP failed to inhibit tumor growth, indicating that the unique mechanism of action of AL008 may be more effective at potentiating the antitumor activity of checkpoint inhibitors than ligand-blocking anti-SIRPα Abs. In summary, AL008 induced SIRPα internalization in vivo and repolarized macrophages toward an antitumoral phenotype that resulted in reduced tumor growth in several models.

Discussion

In the current study, we present a novel, pan-allelic, SIRPα-specific Ab that induces degradation of SIRPα and immune activation of myeloid cells through FcγR2A engagement. AL008 possesses key properties that may convert protumoral TAMs into antitumor effector cells. First, AL008 recognizes a conserved, membrane-proximal epitope

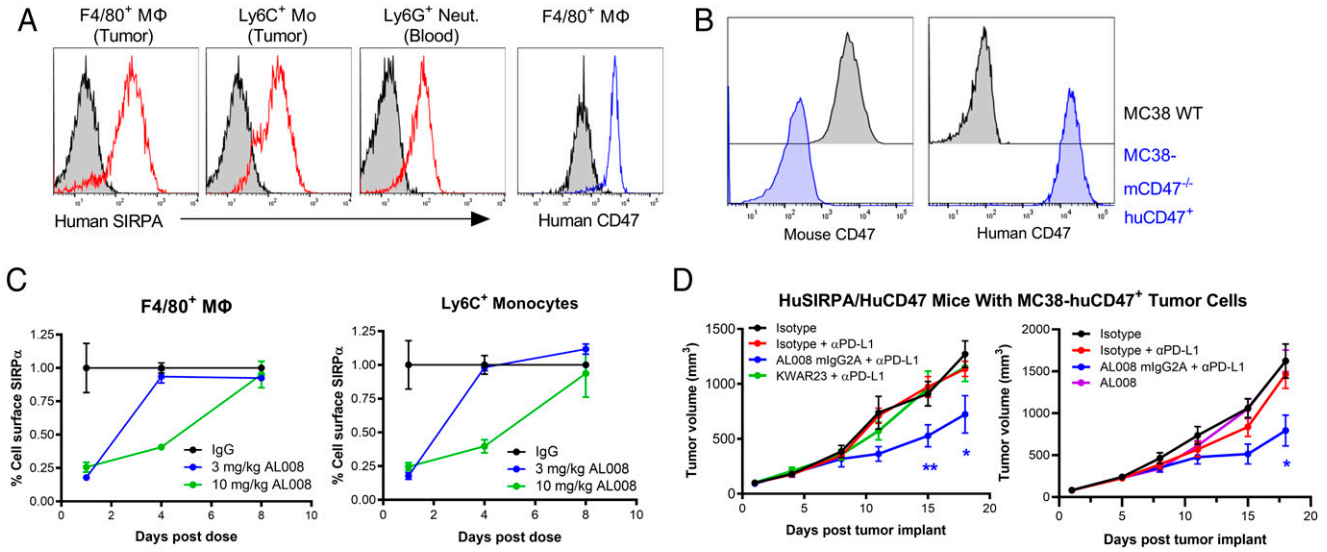

FIGURE 7. AL008 enhances the activity of T cell checkpoint blockade. (**A**) Transgenic mice that express human SIRPα and human CD47 (huSIRPα/huCD47) were generated and implanted with MC38 cells. Expression of huSIRPα on F4/80$^+$ macrophages, Ly6C$^+$ monocytes, and Ly6G$^+$ neutrophils is shown in red. Expression of CD47 on F4/80$^+$ macrophages is shown in blue. (**B**) MC38-huCD47$^+$ cells were generated by deleting mouse CD47 from MC38 cells and expressing a huCD47 by lentivirus transduction. Expression of human and mouse CD47 on WT MC38 (gray) and MC38-huCD47$^+$ (blue) cells is shown. (**C**) huSIRPA/huCD47 mice were implanted with MC38-huCD47 cells and received two doses of 3 mg/kg AL008, 10 mg/kg AL008, or isotype control. On days 1, 4, and 8 postdose, tumors were harvested and dissociated, and myeloid cells were stained for huSIRPα using an anti-SIRPα clone that does not compete with AL008 binding. The percentage of cell surface SIRPα is shown. (**D**) huSIRPα/huCD47 mice were implanted with MC38-huCD47$^+$ cells and treated twice a week for 3 wk with 3 mg/kg anti–PD-L1 + 10 mg/kg mIgG2A, 10 mg/kg AL008 + 3 mg/kg anti–PD-L1, 10 mg/kg KWAR23 + 3 mg/kg anti–PD-L1, 10 mg/kg AL008, or with 3 mg/kg rat IgG2b + 10 mg/kg mIgG2A isotype control. Data are means ± SEM for 9–10 mice per group. The results were replicated, and data from two separate studies are shown. Unpaired Student *t* tests were performed. $*p < 0.05$, $**p < 0.01$.

of SIRPα present in the major allelic variants of SIRPα (v1, v2, v8) but not in SIRPβ or SIRPγ; this unique binding affinity achieves pan-allelic SIRPα reactivity without cross-reacting to other highly homologous SIRP family members. Given the high frequency of SIRPα v2 and v8 across human populations, pan-allele SIRPα binding enables therapeutic targeting of SIRPα in diverse patient populations (23, 42) and would be expected to be more broadly efficacious than v1-specific Abs. AL008 demonstrated a greater ability to stimulate phagocytosis in human macrophages compared with a v1 allele-specific SIRPα Ab (18D5) (10). Furthermore, the ability of AL008 to specifically antagonize SIRPα and not block activating receptors, such as SIRPβ and SIRPγ, provides advantages over cross-reactive SIRP Abs or anti-CD47 Abs. We and others (10, 23, 43) observed this selectivity in dendritic cell–mediated T cell activation MLR assays in which AL008 increased T cell proliferation in comparison with isotype control or a CD47-blocking Ab. The unique combination of broad SIRPα allelic binding and SIRPα specificity provides AL008 with selective advantages compared with first-generation CD47-SIRPα inhibitors.

Second, AL008 has an apparently unique mechanism of action compared with ligand-blocking anti-CD47 or anti-SIRPα Abs (e.g., Refs. 10, 12, 23) in that AL008 induces the internalization of SIRPα from the surface followed by degradation. Whereas anti-SIRPα Abs that competitively block CD47 do not internalize SIRPα, AL008 downregulates surface expression of SIRPα via its unique epitope, which does not overlap with the CD47 binding site. Given the ubiquitous expression of CD47 in both tumor and healthy tissues, clinical efficacy with competitive CD47 blockers requires frequent high doses of drug to saturate receptors. Due to the noncompetitive mechanism of AL008 and the restricted expression of SIRPα to myeloid cells, clinical efficacy with AL008 may require less absolute drug to be administered to patients. An additional advantage of Ab-mediated SIRPα internalization is that other ligands, such as surfactant proteins that bind outside of the CD47-binding domain, are also prevented from interacting with SIRPα. Surfactant proteins A and D are induced in multiple human cancers and have been reported to suppress macrophage phagocytosis (8). Neither CD47-blocking anti-SIRPα Abs that bind the IgV domain of SIRPα nor anti-CD47 Abs would likely be able to block this interaction. The unique mechanism of AL008 to induce SIRPα internalization and degradation without blocking the CD47–SIRPα interaction distinguishes it from first-generation anti-SIRPα Abs.

Lastly, AL008 concurrently engages FcγR2A to provide additional activation signals and facilitate single-agent activity. The family of FcγRs consists of both activating (e.g., FcγR2A) and inhibitory (e.g., FcγR2B) receptors expressed on diverse immune cells and often acts as a central determinant in the function of IgG Abs (39). The role of FcγRs in cancer therapy primarily focuses on antitumor Ag Abs with ADCC activity, which mediate tumor cell killing through FcγR3A on NK cells. However, FcγR2A is the most highly expressed activating FcγR within the myeloid cell lineage (44) and is involved in driving ADCP in macrophages and in the maturation of dendritic cells. In contrast to AL008, the Fc domains of most CD47/SIRPα blockers are attenuated for FcγR-dependent effector function and rely on combination therapies with ADCC molecules to provide the activation signal for enhanced macrophage activity (45, 46). By combining SIRPα inhibition and FcγR stimulation in one molecule, AL008 functions to both "release the brakes" and "step on the accelerator" to induce an antitumor immune response, enabling a potential for monotherapy activity.

Two additional anti-SIRPα Abs, SIRP-1 and SIRP-2, were recently shown to induce macrophage-mediated phagocytosis as single agents (47). SIRP-1 competitively blocks CD47 binding and induces SIRPα internalization, whereas SIRP-2 appears to reduce avid binding to CD47 by disrupting SIRPα dimerization. Unlike SIRP-1, AL008-mediated downregulation of SIRPα leads to degradation of the receptor, which results in long-term removal of SIRPα and elimination of CD47-induced and basal inhibitory signaling in macrophages,

as evidenced by the pharmacodynamic characterization and efficacy of AL008 in tumor models. SIRP-1 and SIRP-2 have also not been shown to bind SIRPα v8, another prominent SIRPα variant that has been shown to occur in ~13–20% of the human population (23). In addition, whereas SIRP-1 and SIRP-2 do not appear to impair T cell proliferation, AL008 stimulates T cell proliferation in the context of dendritic cells, further differentiating AL008 among other published anti-SIRPα Abs.

T cell activation may be of particular relevance in solid tumors. Anti-CD47 Abs were previously reported to suppress T cell activation (10). Accordingly, we observed that in dendritic cell–mediated MLRs, CD47 blockade significantly inhibited T cell proliferation relative to control-treated cells. Furthermore, anti-CD47 Ab treatment partially depleted T cells in vitro and suppressed release of T cell activation cytokines induced by anti–PD-1 (data not shown). In contrast, AL008 significantly increased T cell proliferation in allogeneic MLR assays and did not deplete T cells in vitro or interfere with T cell activation by checkpoint inhibitors. One proposed mechanism for T cell inhibition by anti-CD47 Abs arises from observations that CD47–SIRPγ interaction facilitates cell–cell contact between APCs and T cells (19) and that blockade of this interaction with either anti-CD47 or anti-SIRPγ Abs inhibits T cell activation. Because AL008 does not cross-react with SIRPγ, the stimulatory CD47/SIRPγ axis is preserved. An alternate hypothesis suggests that agonistic anti-CD47 Abs trigger cell-intrinsic inhibitory CD47 signaling to modulate immune responses (48).

In vitro activity of AL008 translated to single-agent and combination effects in the tumor microenvironment. The mechanism of AL008 inducing SIRPα internalization was retained in vivo in TAMs from mice reconstituted with a human immune system or from Tg mice expressing both huSIRPα and huCD47. In addition to SIRPα internalization, AL008 induced TAM activation, inducing the expression of HLA-DR and CD86 in vivo. These markers of M1 macrophage activation suggest repolarization of TAMs toward a proinflammatory phenotype. Consistent with a single-agent effect on pharmacodynamic markers by AL008, we also observed monotherapy efficacy on tumor growth with AL008 in a humanized model. These data are consistent with the dual mechanism of AL008 to promote FcγR activation and block inhibitory receptors through targeting SIRPα. The increased potency of AL008 did not result in increased toxicity in preclinical studies conducted with nonhuman primates or any cell depletion in mice or nonhuman primates (data not shown).

In summary, AL008 is a potentially best-in-class anti-SIRPα mAb with a dual mechanism of action that concurrently induces SIRPα internalization and degradation and FcγR2A activation to provide broad and potent checkpoint inhibition. AL008 is mechanistically differentiated by its pan-allelic, SIRPα-specific epitope that induces single-agent and combination phagocytic activity, reduces tumor growth in vivo, and promotes dendritic cell–mediated T cell activation. These data support the advancement of AL008 toward early clinical development.

Acknowledgments

Editorial support and publication assistance were provided by SCIENT Healthcare Communications (Cedar Knolls, NJ).

Disclosures

This work was supported by Alector, Inc. A.P., W.-H.H., and A.R. are authors of patents related to SIRPα. A.P. and A.R. are named inventors on International Patent Application Publication No. WO2018/107058; A.P., W.-H.H., and A.R. are named inventors on International Patent Application Publication No. WO2019/226973 and U.S. Patent No. 11,319,373. All authors are shareholders of Alector LLC, a company developing SIRPα antagonists.

References

1. DeNardo, D. G., and B. Ruffell. 2019. Macrophages as regulators of tumour immunity and immunotherapy. *Nat. Rev. Immunol.* 19: 369–382.
2. Gordon, S., and P. R. Taylor. 2005. Monocyte and macrophage heterogeneity. *Nat. Rev. Immunol.* 5: 953–964.
3. Gordon, S., and F. O. Martinez. 2010. Alternative activation of macrophages: mechanism and functions. *Immunity* 32: 593–604.
4. Barclay, A. N., and M. H. Brown. 2006. The SIRP family of receptors and immune regulation. *Nat. Rev. Immunol.* 6: 457–464.
5. Willingham, S. B., J. P. Volkmer, A. J. Gentles, D. Sahoo, P. Dalerba, S. S. Mitra, J. Wang, H. Contreras-Trujillo, R. Martin, J. D. Cohen, et al. 2012. The CD47-signal regulatory protein alpha (SIRPa) interaction is a therapeutic target for human solid tumors. *Proc. Natl. Acad. Sci. USA* 109: 6662–6667.
6. Jaiswal, S., C. H. Jamieson, W. W. Pang, C. Y. Park, M. P. Chao, R. Majeti, D. Traver, N. van Rooijen, and I. L. Weissman. 2009. CD47 is upregulated on circulating hematopoietic stem cells and leukemia cells to avoid phagocytosis. *Cell* 138: 271–285.
7. Barclay, A. N., and T. K. Van den Berg. 2014. The interaction between signal regulatory protein alpha (SIRPα) and CD47: structure, function, and therapeutic target. *Annu. Rev. Immunol.* 32: 25–50.
8. Janssen, W. J., K. A. McPhillips, M. G. Dickinson, D. J. Linderman, K. Morimoto, Y. Q. Xiao, K. M. Oldham, R. W. Vandivier, P. M. Henson, and S. J. Gardai. 2008. Surfactant proteins A and D suppress alveolar macrophage phagocytosis via interaction with SIRPα. *Am. J. Respir. Crit. Care Med.* 178: 158–167.
9. Chao, M. P., A. A. Alizadeh, C. Tang, J. H. Myklebust, B. Varghese, S. Gill, M. Jan, A. C. Cha, C. K. Chan, B. T. Tan, et al. 2010. Anti-CD47 antibody synergizes with rituximab to promote phagocytosis and eradicate non-Hodgkin lymphoma. *Cell* 142: 699–713.
10. Gauttier, V., S. Pengam, J. Durand, K. Biteau, C. Mary, A. Morello, M. Néel, G. Porto, G. Teppaz, V. Thepenier, et al. 2020. Selective SIRPα blockade reverses tumor T cell exclusion and overcomes cancer immunotherapy resistance. *J. Clin. Invest.* 130: 6109–6123.
11. Liu, J., L. Wang, F. Zhao, S. Tseng, C. Narayanan, L. Shura, S. Willingham, M. Howard, S. Prohaska, J. Volkmer, et al. 2015. Pre-clinical development of a humanized anti-CD47 antibody with anti-cancer therapeutic potential. *PLoS One* 10: e0137345.
12. Liu, J., S. Xavy, S. Mihardja, S. Chen, K. Sompalli, D. Feng, T. Choi, B. Agoram, R. Majeti, I. L. Weissman, and J. P. Volkmer. 2020. Targeting macrophage checkpoint inhibitor SIRPα for anticancer therapy. *JCI Insight* 5: e134728.
13. Advani, R., I. Flinn, L. Popplewell, A. Forero, N. L. Bartlett, N. Ghosh, J. Kline, M. Roschewski, A. LaCasce, G. P. Collins, et al. 2018. CD47 blockade by Hu5F9-G4 and rituximab in non-Hodgkin's lymphoma. *N. Engl. J. Med.* 379: 1711–1721.
14. Sikic, B. I., N. Lakhani, A. Patnaik, S. A. Shah, S. R. Chandana, D. Rasco, A. D. Colevas, T. O'Rourke, S. Narayanan, K. Papadopoulos, et al. 2019. First-in-human, first-in-class phase I trial of the anti-CD47 antibody Hu5F9-G4 in patients with advanced cancers. *J. Clin. Oncol.* 37: 946–953.
15. Abrisqueta, P., J. Sancho, R. Cordoba, D. Persky, C. Andreadis, S. Huntington, C. Carpio, D. M. Giles, X.-X. Wei, Y. F. Li, et al. 2019. Anti-CD47 antibody, CC-90002, in combination with rituximab in subjects with relapsed and/or refractory non-Hodgkin lymphoma (R/R NHL). *Blood* 134(Suppl. 1): 4089.
16. Patnaik, A., A. Spreafico, A. M. Paterson, M. Peluso, J.-K. Chung, B. Bowers, D. Niforos, A. M. O'Neill, M. Beeram, M. Iafolla, et al. 2020. Results of a first-in-human phase I study of SRF231, a fully human, high-affinity anti-CD47 antibody. *J. Clin. Oncol.* 38(15 Suppl.): 3064.
17. Piccio, L., W. Vermi, K. S. Boles, A. Fuchs, C. A. Strader, F. Facchetti, M. Cella, and M. Colonna. 2005. Adhesion of human T cells to antigen-presenting cells through SIRPβ2-CD47 interaction costimulates T-cell proliferation. *Blood* 105: 2421–2427.
18. Brooke, G., J. D. Holbrook, M. H. Brown, and A. N. Barclay. 2004. Human lymphocytes interact directly with CD47 through a novel member of the signal regulatory protein (SIRP) family. *J. Immunol.* 173: 2562–2570.
19. Stefanidakis, M., G. Newton, W. Y. Lee, C. A. Parkos, and F. W. Luscinskas. 2008. Endothelial CD47 interaction with SIRPγ is required for human T-cell transendothelial migration under shear flow conditions in vitro. *Blood* 112: 1280–1289.
20. Adams, S., L. J. van der Laan, E. Vernon-Wilson, C. Renardel de Lavalette, E. A. Döpp, C. D. Dijkstra, D. L. Simmons, and T. K. van den Berg. 1998. Signal-regulatory protein is selectively expressed by myeloid and neuronal cells. *J. Immunol.* 161: 1853–1859.
21. Takenaka, K., T. K. Prasolava, J. C. Wang, S. M. Mortin-Toth, S. Khalouei, O. I. Gan, J. E. Dick, and J. S. Danska. 2007. Polymorphism in Sirpa modulates engraftment of human hematopoietic stem cells. *Nat. Immunol.* 8: 1313–1323.
22. Treffers, L. W., X. W. Zhao, J. van der Heijden, S. Q. Nagelkerke, D. J. van Rees, P. Gonzalez, J. Geissler, P. Verkuijlen, M. van Houdt, M. de Boer, et al. 2018. Genetic variation of human neutrophil Fcγ receptors and SIRPα in antibody-dependent cellular cytotoxicity towards cancer cells. *Eur. J. Immunol.* 48: 344–354.
23. Voets, E., M. Paradé, D. Lutje Hulsik, S. Spijkers, W. Janssen, J. Rens, I. Reinieren-Beeren, G. van den Tillaart, S. van Duijnhoven, L. Driessen, et al. 2019. Functional characterization of the selective pan-allele anti-SIRPα antibody ADU-1805 that blocks the SIRPα-CD47 innate immune checkpoint. *J. Immunother. Cancer* 7: 340.
24. Pons, J., B. J. Sim, H. Wan, T. C.-C. Kuo, S. E. Kauder, W. D. Harriman, and S. Izquierdo. Antibodies against signal-regulatory protein alpha and methods of use. International patent application PCT/US2017/052592, Publication No. WO/2018/057669. 2018 Mar 29.
25. Poirier, N., C. Mary, B. Vanhove, V. Gauttier, V. Thepenier, and S. Pengam. New anti-SIRPa antibodies and their therapeutic applications. International patent application PCT/EP2017/059071, Publication No. WO/2017/178653. 2017 Oct 19.
26. Davidson, E., and B. J. Doranz. 2014. A high-throughput shotgun mutagenesis approach to mapping B-cell antibody epitopes. *Immunology* 143: 13–20.

27. Munn, D. H., and N. K. Cheung. 1987. Interleukin-2 enhancement of monoclonal antibody-mediated cellular cytotoxicity against human melanoma. *Cancer Res.* 47: 6600–6605.
28. Crowe, J. S., V. S. Hall, M. A. Smith, H. J. Cooper, and J. P. Tite. 1992. Humanized monoclonal antibody CAMPATH-1H: myeloma cell expression of genomic constructs, nucleotide sequence of cDNA constructs and comparison of effector mechanisms of myeloma and Chinese hamster ovary cell-derived material. *Clin. Exp. Immunol.* 87: 105–110.
29. Ring, N. G., D. Herndler-Brandstetter, K. Weiskopf, L. Shan, J. P. Volkmer, B. M. George, M. Lietzenmayer, K. M. McKenna, T. J. Naik, A. McCarty, et al. 2017. Anti-SIRPα antibody immunotherapy enhances neutrophil and macrophage antitumor activity. *Proc. Natl. Acad. Sci. USA* 114: E10578–E10585.
30. Londino, J. D., D. Gulick, J. S. Isenberg, and R. K. Mallampalli. 2015. Cleavage of signal regulatory protein α (SIRPα) enhances inflammatory signaling. *J. Biol. Chem.* 290: 31113–31125.
31. Waclavicek, M., O. Majdic, T. Stulnig, M. Berger, T. Baumruker, W. Knapp, and W. F. Pickl. 1997. T cell stimulation via CD47: agonistic and antagonistic effects of CD47 monoclonal antibody 1/1A4. *J. Immunol.* 159: 5345–5354.
32. Seiffert, M., P. Brossart, C. Cant, M. Cella, M. Colonna, W. Brugger, L. Kanz, A. Ullrich, and H. J. Bühring. 2001. Signal-regulatory protein α (SIRPα) but not SIRPβ is involved in T-cell activation, binds to CD47 with high affinity, and is expressed on immature $CD34^+CD38^-$ hematopoietic cells. *Blood* 97: 2741–2749.
33. Shang, L., B. Daubeuf, M. Triantafilou, R. Olden, F. Dépis, A. C. Raby, S. Herren, A. Dos Santos, P. Malinge, I. Dunn-Siegrist, et al. 2014. Selective antibody intervention of Toll-like receptor 4 activation through Fc γ receptor tethering. *J. Biol. Chem.* 289: 15309–15318.
34. Hezareh, M., A. J. Hessell, R. C. Jensen, J. G. van de Winkel, and P. W. Parren. 2001. Effector function activities of a panel of mutants of a broadly neutralizing antibody against human immunodeficiency virus type 1. *J. Virol.* 75: 12161–12168.
35. Xu, D., M. L. Alegre, S. S. Varga, A. L. Rothermel, A. M. Collins, V. L. Pulito, L. S. Hanna, K. P. Dolan, P. W. Parren, J. A. Bluestone, et al. 2000. In vitro characterization of five humanized OKT3 effector function variant antibodies. *Cell. Immunol.* 200: 16–26.
36. Vaughan, A. T., C. H. Chan, C. Klein, M. J. Glennie, S. A. Beers, and M. S. Cragg. 2015. Activatory and inhibitory Fcγ receptors augment rituximab-mediated internalization of CD20 independent of signaling via the cytoplasmic domain. *J. Biol. Chem.* 290: 5424–5437.
37. Hubbard, J. J., M. Pyzik, T. Rath, L. K. Kozicky, K. M. K. Sand, A. K. Gandhi, A. Grevys, S. Foss, S. C. Menzies, J. N. Glickman, et al. 2020. FcRn is a CD32a coreceptor that determines susceptibility to IgG immune complex-driven autoimmunity. *J. Exp. Med.* 217: e20200359.
38. Bengtsson, A. A., H. Tyden, and C. Lood. 2020. Neutrophil FcγRIIA availability is associated with disease activity in systemic lupus erythematosus. *Arthritis Res. Ther.* 22: 126.
39. Guilliams, M., P. Bruhns, Y. Saeys, H. Hammad, and B. N. Lambrecht. 2014. The function of Fcγ receptors in dendritic cells and macrophages. [Published erratum appears in 2014 *Nat. Rev. Immunol.* 14: 340.] *Nat. Rev. Immunol.* 14: 94–108.
40. Means, T. K., E. Latz, F. Hayashi, M. R. Murali, D. T. Golenbock, and A. D. Luster. 2005. Human lupus autoantibody-DNA complexes activate DCs through cooperation of CD32 and TLR9. *J. Clin. Invest.* 115: 407–417.
41. Ambarus, C. A., S. Krausz, M. van Eijk, J. Hamann, T. R. Radstake, K. A. Reedquist, P. P. Tak, and D. L. Baeten. 2012. Systematic validation of specific phenotypic markers for in vitro polarized human macrophages. *J. Immunol. Methods* 375: 196–206.
42. Sim, J., J. T. Sockolosky, E. Sangalang, S. Izquierdo, D. Pedersen, W. Harriman, A. S. Wibowo, J. Carter, A. Madan, L. Doyle, et al. 2019. Discovery of high affinity, pan-allelic, and pan-mammalian reactive antibodies against the myeloid checkpoint receptor SIRPα. *MAbs* 11: 1036–1052.
43. Dehmani, S., V. Nerrière-Daguin, M. Néel, N. Elain-Duret, J.-M. Heslan, L. Belarif, C. Mary, V. Thepenier, K. Biteau, N. Poirier, et al. 2021. SIRPγ-CD47 interaction positively regulates the activation of human T cells in situation of chronic stimulation. *Front. Immunol.* 12: 732530.
44. Hogarth, P. M., and G. A. Pietersz. 2012. Fc receptor-targeted therapies for the treatment of inflammation, cancer and beyond. *Nat. Rev. Drug Discov.* 11: 311–331.
45. Kauder, S. E., T. C. Kuo, O. Harrabi, A. Chen, E. Sangalang, L. Doyle, S. S. Rocha, S. Bollini, B. Han, J. Sim, et al. 2018. ALX148 blocks CD47 and enhances innate and adaptive antitumor immunity with a favorable safety profile. *PLoS One* 13: e0201832.
46. Weiskopf, K., A. M. Ring, C. C. Ho, J. P. Volkmer, A. M. Levin, A. K. Volkmer, E. Ozkan, N. B. Fernhoff, M. van de Rijn, I. L. Weissman, and K. C. Garcia. 2013. Engineered SIRPα variants as immunotherapeutic adjuvants to anticancer antibodies. *Science* 341: 88–91.
47. Andrejeva, G., B. J. Capoccia, R. R. Hiebsch, M. J. Donio, I. M. Darwech, R. J. Puro, and D. S. Pereira. 2021. Novel SIRPα antibodies that induce single-agent phagocytosis of tumor cells while preserving T cells. *J. Immunol.* 206: 712–721.
48. Grimbert, P., S. Bouguermouh, N. Baba, T. Nakajima, Z. Allakhverdi, D. Braun, H. Saito, M. Rubio, G. Delespesse, and M. Sarfati. 2006. Thrombospondin/CD47 interaction: a pathway to generate regulatory T cells from human $CD4^+CD25^-$ T cells in response to inflammation. *J. Immunol.* 177: 3534–3541.